Atmospheric Environment 310 (2023) 119966

Contents lists available at ScienceDirect

Atmospheric Environment

journal homepage: www.elsevier.com/locate/atmosenv

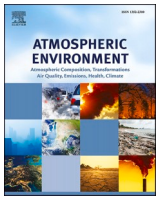

Multi-year total ozone column variability at three Norwegian sites and the influence of Northern Hemisphere Climatic indices

Giulia Boccacci [a], Chiara Bertolin [b], Stefano Cavazzani [b], Anna Maria Siani [c,*]

[a] Department of Earth Sciences, Sapienza University of Rome, P.le Aldo Moro, 5, 00185, Rome, Italy
[b] Department of Mechanical and Industrial Engineering, Norwegian University of Science and Technology, Richard Birkelands vei 2B, 7491, Trondheim, Norway
[c] Department of Physics, Sapienza University of Rome, P.le Aldo Moro, 5, 00185, Rome, Italy

HIGHLIGHTS

- Total ozone column trends investigation through satellite data analysis.
- Geopotential height represents a fingerprint of total ozone variability.
- Teleconnection indices illustrate total ozone column regional differences.
- Prominent role of SCAND index at northern latitudes locations of Andøya and Trondheim.
- No significant total ozone anomaly events in Oslo during increasing solar variation.

ARTICLE INFO

Keywords:
Total ozone column
Geopotential height
Remote sensing
NAO index
AO index
SCAND index

ABSTRACT

Total ozone column (TOC) measurements are retrieved from the Ozone Monitoring Instrument (OMI) onboard the NASA Earth Observing System (EOS) Aura satellite at the three Norwegian sites: Oslo (59.9°N 10.7°E, 1 m a.s.l.), Trondheim (63.4°N 10.4°E, 3 m a.s.l.) and Andøya (69.1°N 15.7°E, 32 m a.s.l.). TOC data have been analysed from 2005 to 2021, in order to detect annual and multi-years total ozone variability. The relationship between geopotential height (GPH) at 250 hPa and total ozone column has been evaluated after showing that monthly anomalies in GPH and TOC are correlated amongst the three sites. The influence of the three Northern Hemisphere Tele Connection (TC) indices (North Atlantic Oscillation, Arctic Oscillation and Scandinavia) on TOC variability has been investigated. It is found that Scandinavia index plays a prominent role for the northernmost latitudes of Andøya and Trondheim while North Atlantic Oscillation and Arctic Oscillation indices are weakly correlated (negatively) to TOC and (positively) to GPH at Oslo. The response of TOC variability to the solar activity at the three sites is also explored and it is noticed that in the period of increasing variation of solar activity, significant TOC anomaly events are only observed in Andøya and Trondheim.

1. Introduction

The global distribution of total ozone is explained by photochemical processes involving the solar ultraviolet radiation and the air motions related to weather systems and the e-scale Brewer-Dobson circulation (Solomon, 1999; World Meteorological Organization United States, 2018; Petkov et al., 2014, 2023; Maria et al., 2002; Weber et al., 2011; Brönnimann, 2022). Since the early studies changes in the amount of total ozone can be linked to changes in tropopause altitude (Dobson and Harrison, 1926; Steinbrecht et al., 1998). Fountoulakis et al. (2021) confirmed the findings of previous studies on the role played by tropospheric dynamics on total ozone variability, showing a strong and statistically significant anticorrelation between total ozone and geopotential height at 250 hPa GPH at the three Italian stations examined and for all the seasons.

In addition, several studies have related the behaviour and geographical distribution of some climatic modes (i.e., Quasi-Biennial Oscillation (QBO), North Atlantic Oscillation (NAO), Arctic Oscillation (AO), etc.) to the evolution of ozone column in a wide range of temporal and spatial scales. Monge-Sanz et al. (2003) showed a strong correlation

* Corresponding author.
E-mail addresses: giulia.boccacci@uniroma1.it (G. Boccacci), chiara.bertolin@ntnu.no (C. Bertolin), stefano.cavazzani@ntnu.no (S. Cavazzani), annamaria.siani@uniroma1.it (A.M. Siani).

https://doi.org/10.1016/j.atmosenv.2023.119966
Received 12 April 2023; Received in revised form 14 July 2023; Accepted 17 July 2023
Available online 19 July 2023

between total ozone decrease and the North Atlantic Oscillation and Arctic Oscillation indices over south-western European locations. Observations for the El Niño winter 1987 show a negative North Atlantic Oscillation index with corresponding changes in temperature and precipitation patterns, a weak polar vortex, a warm Arctic middle stratosphere and negative total ozone anomalies in the tropics together with positive total ozone anomalies at middle to high latitudes (Brönnimann et al., 2006). Climate patterns can affect ozone on a broad spectrum, and it is therefore fundamental to consider their potential effect in different regions and seasons (Ossó et al., 2011). Koo et al. (2014) investigated the regional climate variability influence on the arctic ozone depletion events (ODE) through five different teleconnection indices and found that the Western Pacific (WP) can be used to diagnose ODE changes (i.e., interannual variability) and subsequent environmental impacts in the Arctic spring. At the same time, historical total ozone column data on an interannual time scale, can help to shed light on the variability of the stratospheric circulation, as in the case of Brönnimann et al. (Brönnimann, 2022). The authors found that the 1940–1942 total ozone column exceptional anomalies recorded in Oxford, can be explained by atmospheric circulation. Specifically, the underlying cause of the strong Brewer-Dobson circulation (resulting in an increased transport of ozone from the tropics to the extratropic), was an El Niño event, accompanied by a strong positive Pacific North American (PNA) pattern and a negative phase of the North Atlantic Oscillation (NAO).

Regarding higher latitudes regions of the northern hemisphere (and specifically Norway), the 65-year total ozone record from Tromsø has been analysed by Hansen et al. (Hansen and Svenøe, 2005), that found a complex contribution of teleconnection indices (with no single index being persistently dominant over several months). The variability of teleconnection terms is probably caused by the changing influence of air masses on the local tropopause altitude, with a dominant influence of North Atlantic and Arctic indices in winter/spring, and of lower-latitude ones in summer and early autumn. Svendby et al. (Svendby, 2004) analysed total ozone data from Oslo (Norway) over the period 1978 to 1998. In this study, eight different teleconnection indices (North Atlantic Oscillation, East Atlantic Oscillation, East Atlantic Jet pattern, East Atlantic/West Russia pattern, Scandinavia pattern, Polar/Eurasia pattern, West Pacific pattern and the Pacific/North American pattern) were considered and it was found that all of them, except from Scandinavia and Polar/Eurasia pattern, were significant in explaining stratospheric variability in Oslo. Total ozone column over the northern polar cap (latitudes >63°N) was exceptionally low in late winter and early spring (February–April) of 2020 (Lawrence et al., 2020; Petkov et al., 2021) and this was partially due to an exceptionally strong, cold, and persistent stratospheric polar vortex, which provided ideal conditions for chemical ozone destruction to occur (Grooß and Müller, 2022; Wohltmann et al., 2020; Manney et al., 2020). Global total ozone trends from ground-based and satellite data including polar regions have been extensively investigated by Weber et al., 2018, 2022, but regional differences were not addressed. Bernet et al. (2023) investigated regional total ozone trends from ground-based measurements at three northern high-latitude stations in Norway and defined a set of predictors that explain the natural ozone variability at the three stations in the best possible way. Absorption of incoming UV radiation is also a crucial mechanism for stratospheric ozone formation and affects ozone amounts. The 11-year solar cycle dominates the incoming UV radiation and has been identified in many ozone records (Knibbe et al., 2014). A commonly used proxy to characterize the UV radiation in ozone studies is the 10.7 cm solar flux data, provided as a service by the National Research Council of Canada.

The present research analyses investigate the total ozone column data retrieved from satellite measurements at three Norwegian sites located in the region ranging 60°–69° north latitude: Oslo, Trondheim and Andøya. To the best of our knowledge, the total ozone in Norwegian area was not particularly studied in relation to circulation indices and even less by using satellite data. Moreover, no previous studies attempted to explore the existing relationship between total ozone and geopotential height satellite data to compare regional differences within Norway. Therefore, a comprehensive evaluation of the possible interactions between the geopotential height at 250 hPa, the Northern Hemisphere teleconnection indices, and the solar activity can provide useful insights on multi-year total ozone column variability.

2. Datasets and methodology

2.1. Total ozone column (TOC) and geopotential heights (GPH) at three Norwegian sites

The total ozone column (TOC) daily data for the period 2005–2021 have been provided from the Ozone Monitoring Instrument (OMI) flying on the NASA polar satellite Aura, which has an orbit inclined of 98.22° and a period of 98.83 min (perigee of 708 km and apogee of 710 km). Aura's Ozone Monitoring Instrument (OMI) uses imaging to observe solar back scattered visible and ultraviolet radiation with an area that provides global coverage with a spatial resolution of 13 × 24 km^2. The spatial resolution used in this work is 0. 25° × 0.25°, corresponding to 27.5 × 27.5 km. Two algorithms OMI-TOMS (Total Ozone Mapping Spectrometer) and OMI-DOAS (Differential Optical Absorption Spectroscopy) are used to produce daily TOC values. In this study, the Level 3 Total Column Ozone Global Product is used, based on the Differential Absorption Spectroscopy (DOAS) fitting technique, which essentially uses OMI visible radiance values between 331.1 and 336.1 nm. TOC data have been retrieved for three different Norwegian sites, located at different latitudes: Oslo [59.9°N 10.7°E, 1 m a.s.l.], Trondheim [63.4°N 10.4°E, 3 m a.s.l.] and Andøya [69.1°N 15.7°E, 32 m a.s.l.] (Fig. 1).

Daily means of total ozone were used for the calculation of monthly averages, for months for which measurements were available for at least 15 days. Because of the location of Andøya at 69.1°N, the Sun is below the horizon from 29 November to 13 January (Weather Spark Available online, 1483). No data over this time of the year exist and for this reason, the months of December and January were not included in the analysis for this site, while the month of November was included, but its monthly average was calculated on less daily data (29 days instead of 30 days) than the other two locations (Oslo and Trondheim) which have full data yearly coverage. Moreover, different ozone retrieval algorithms have been used over the years, which have gradually improved the quality and confidence of ozone data derived from satellite measurements. Corrections for instrumental drift and increased knowledge of ozone absorption cross sections as well as latitude-dependent atmospheric profiles have improved the data quality, especially in the Polar regions (Svendby et al., 2021).

The connection between TOC and tropopause height was already recognized since the pioneering studies (Dobson and Harrison, 1926; Vaughan G, 1991) and has been well explored in subsequent studies (Fountoulakis et al., 2021; Liu et al., 2020; Okoro et al., 2021). In the present research daily data of geopotential heights at 250 hPa (hereafter named GPH unless otherwise specified) have been used as it was found (Fountoulakis et al., 2021) to have strong anticorrelation with tropopause height (related to weather scale phenomena reflect in the changes in the height of the tropopause), hence, to be a fingerprint of total ozone variability related to the dynamical tropospheric processes. Geopotential height data analysed here for the period 2005–2021 are provided for the same three Norwegian sites by the Atmospheric Infrared Sounder (AIRS) which is a grating spectrometer aboard Earth Observing System (EOS)-Aqua. In this case the spatial resolution used for all of the three different sites, is 1.0° × 1.0°. Aqua is a near polar sun-synchronous orbit satellite (altitude 705 km, inclination 98.2°, and period 98.8 min) (GIOVANNI, 2023). The satellite data are extracted with Geospatial Interactive Online Visualization And aNalysis Infrastructure (GIOVANNI) a Web-based application developed by the Goddard Earth Sciences Data and Information Services Center (GES DISC). GPH are derived from AIRS Level 3 Standard Products (AIRS, 2019) that

Fig. 1. Topographic map of Norway and the three sites under study (Oslo [59.9°N 10.7°E, 1 m a.s.l.], Trondheim [63.4°N 10.4°E, 3 m a.s.l.] and Andøya [69.1°N 15.7°E, 32 m a.s.l.]).

comprise 24 levels that can be extracted between 1 and 1000 hPa through GIOVANNI's data analysis platform (GIOVANNI, 2023). The retrieval of AIRS GPH is described in (Susskind et al., 2003; Schwartz et al., 2008). Geopotential heights are derived by integrating up through the atmosphere from the surface, therefore the quality at all levels of the atmosphere is only good when the quality of both temperature and water vapor is good near the surface (Tian et al., 2020).

2.2. Teleconnection (TC) indices

The North Atlantic Oscillation Index, Arctic Oscillation Index, and Scandinavia Index were selected among the most dominant modes of climate variability in the Northern Hemisphere, especially at high latitudes, to explore their associations with total ozone column trend over time. In this study, all the climate indices on monthly basis were extracted from the NOAA Climate Prediction Center (Climate Prediction Center, 2023), for the period 2005–2021.

The North Atlantic Oscillation (NAO) Index is recognized as the main synoptic mode of variability of atmospheric circulation over the North Atlantic and affecting European winter climate; it is defined as the difference between the surface pressure related to Subtropical (Azores) High and the Iceland low-pressure systems (Hurrell et al., 2003). NAO ranges between positive and negative index values. It is well correlated with the mean tropopause pressure over the Northern latitudes in the Atlantic European region (Appenzeller et al., 2000), therefore an anti-correlation between NAO and total ozone can be expected. It has been found by Osso et al. (Ossó et al., 2011), that TOC variability associated with the NAO is particularly important during winter over northern Europe, explaining up to 30% in TOC variance for this region. The influence of this climatic modes was also explored over the Iberian Peninsula by Mateos et al. (2015) who assessed that the NAO pattern can explain more than 20% of the annual TOC variability. High levels of TOC observed during 2010 in the northern hemisphere were attributed to a pronounced and persistent negative phase of the North Atlantic and Arctic Oscillations (Steinbrecht et al., 2011).

The Arctic Oscillation (AO) has the dominant role for the climate variability in the northern hemisphere and is an indication of varying interaction between the mid-to-high latitudes and the Arctic, (Thompson and Wallace, 1998; Creilson et al., 2005). The AO variability is essentially an indication of changes in the polar vortex, that is strengthened (weakened) when AO has a positive (negative) phase (Baldwin and Dunkerton, 1979). As already stated for the NAO index, also the AO ranges between positive and negative values. It was found by Liu et al. (2020) that the interannual relationship between AO and ozone in the stratosphere over the Arctic exhibits sub-seasonal variations, and it may provide some information to better predict the potential ozone recovery over Arctic. Recently, Zhang et al. (2017) further showed the close link between AO and ozone after analysing the influence of AO on the vertical distribution of stratospheric ozone in the northern hemisphere in winter. In addition, other studies have noted that there is a significant AO signal in the TOC evolution that is manifested mainly in stratospheric ozone and this implies a strong effect of the AO on the stratospheric ozone distribution (Steinbrecht et al., 2011; Schnadt and Dameris, 2003).

The Scandinavia (SCAND) Index consists of a primary circulation centre over Scandinavia, with weaker centres of opposite sign over

western Europe and eastern Russia/western Mongolia. It has been previously referred to as the Eurasia-1 pattern by (Barnston, 1987). The SCAND ranges between positive and negative index values: the positive phase is associated with positive height anomalies, sometimes reflecting major blocking anticyclones, over Scandinavia and western Russia, while the negative phase of the pattern is associated with negative anomalies in these regions (Climate Prediction Center, 2023). SCAND index was analysed by Orsolini et al. (Orsolini and Doblas-Reyes, 2003) together with other leading climate patterns, in order to derive their signatures in the ozone behaviour. In the study conducted by Svendby et al. (Svendby, 2004) on ozone data from 1978 to 1998 in Oslo (Norway), it was confirmed that SCAND is barely correlated to total ozone variations.

2.3. Solar radio flux (SRF)

As a proxy of solar activity, we analysed the Solar Radio Flux (SRF) at 10.7 cm (also known as F10.7 Index expressed in sfu), which is generally employed as a good indicator for solar-terrestrial investigations (Tapping, 2013). For this purpose, monthly data were derived from National Research Council Canada (Solar Radio Flux, 2023) or the period 2005–2021, approximately spanning from solar cycles 23 to 24. The F10.7 well correlates with the sunspot number as well as with a number of UltraViolet (UV) and visible solar irradiance records. It was used in this study to investigate the combined influence of the solar activity and TC indices on total ozone column.

2.4. Data preprocessing and analysis

At first, the TOC data series retrieved from OMI-TOMS and OMI-DOAS were evaluated in term of their completeness through the Completeness Index (CoI) (Frasca et al., 2017). The index ranges between 0 (no measurements, all data discarded for instrumental problems) and unity (no missing values). CoI index for Andøya was computed by considering a lower total number of the series (i.e., 5423 observations instead of 6205) with respect to Oslo and Trondheim, due to the lack of data collection over the above-mentioned dark period (i.e., 29 November – 13 January of each year).

Secondly, standardized seasonal anomalies of TOC and GPH have been computed for each different station, by calculating seasonal averages on three months of daily data (December, January and February for winter; March, April and May for spring; June, July and August for summer and September, October and November for autumn). Then, multi-year seasonal mean has been subtracted from the seasonal average values of each year and the difference was divided by their standard deviation. A *period of interest* has been lately selected based on the higher ozone variability over the whole-time span. Standardized seasonal TOC and GPH anomalies have been compared to analyse their correlation over the considered period of interest.

Later on, in order to gain more insights on the evolution of the atmospheric parameters at each different station over the considered years, daily means of total ozone and geopotential height were used for the calculation of monthly averages, for months for which measurements were available for at least 15 days (with the sub-criterion that measurements were available for at least 5 days for each of the following sub-periods: day 1–day 10, day 11–day 20, day 21– end). In all cases, multi-year monthly means of each quantity were also calculated for the whole selected period. Monthly anomalies were then computed by subtracting the multi-year monthly means from the monthly average values and the values were subsequently standardized by dividing the difference by the standard deviation (the same procedure was applied independently for each of the three different sites). Thanks to this procedure, the influence of geopotential height at 250 hPa on total ozone behaviour has been explored examining Pearson correlations between the selected sites both in terms of TOC and GPH anomalies, to assess if they have been affected by the same synoptical systems. After that, a specific criterion has been chosen with the purpose of gaining insight on the occurrences of significant TOC and GPH anomaly events at high-latitude: the standardized TOC and GPH monthly anomaly events have been considered as "significant" only when exceed $+1\sigma$ or are lower than -1σ. Very high anomalous events have also been underlined by filtering the data respectively above and below a $\pm 2\sigma$ threshold.

Finally, the connection between total ozone column and teleconnection indices has been also investigated by exploring the existing correlations between the two parameters, also considering the geopotential height at 250 hPa. The Spearman coefficient was used in this regard in order to assess how well the relationship among the above-mentioned variables can be described using a monotonic function, without then assuming linearity in the correlation.

Solar activity has also been explored by analysing the Solar Radio Flux (s.f.u.) over the whole period (2005–2021) with the purpose of understanding its influence on the teleconnection indices' variability, and on the relationship between TOC and GPH time behaviour over the Norwegian area.

3. Results and discussion

3.1. Data preprocessing

The Completeness (CoI) index obtained for each location and for each of the two OMI products (TOMS and DOAS) is shown in Table 1. The CoI values result higher for the OMI-DOAS product therefore this dataset has been selected for subsequent data analyses. This index has been here used as an exploratory tool in order to assess if data availability was enough to compute monthly means (with the aim of subsequently work with monthly anomalies). Indeed, a lower coverage of data would not have allowed the calculation of monthly and seasonal anomalies that were actually significant to conduct the investigations reported in next paragraphs.

Fig. 2 shows the TOC anomalies behaviour for the three sites on a seasonal basis. Maximum decrease in total ozone column is observed in spring 2011 for the city of Andøya (green line in Fig. 2), as already confirmed by the study on the severe depletion affected the Arctic area in 2011 (Manney et al., 2011) due to the weather conditions that led to stratospheric temperatures lower than average (during the winter period) and stronger polar vortex. The effect is also visible at the lower latitudes of Trondheim and Oslo. Similarly, the significant ozone reduction was also experienced at lower mid-latitudes sites in Europe (Petkov et al., 2014). These conditions inhibited transport of ozone-rich air to high latitudes and facilitated severe chemical depletion of ozone (World Meteorological Organization United States, 2018).

Other severe ozone depleted winter is 2016 for both the city of Oslo and Trondheim (no data available for Andøya) when Arctic temperatures were the lowest in at least 68 years (Matthias et al., 2016), and ozone dropped more rapidly than in 2010/2011 (Manney and Lawrence, 2016). The critical factor resulting in less ozone loss than in 2011 was the major final warming occurred in early March 2016 that halted chemical processing and dispersed processed air from the vortex

Table 1
Completeness Index (CoI) for Total Ozone Column satellite data from OMI-TOMS ad OMI-DOAS products in the time span between 01 and 01–2005 and 31-12-2021.

Site	OMI Product	CoI
Trondheim	TOMS	0.82
	DOAS	0.94
Oslo	TOMS	0.93
	DOAS	0.96
Andøya	TOMS	0.81[a]
	DOAS	0.89[a]

[a] Computed by considering 5423 total number of observations instead of 6205 (no data available from 29 November to 13 January of each year).

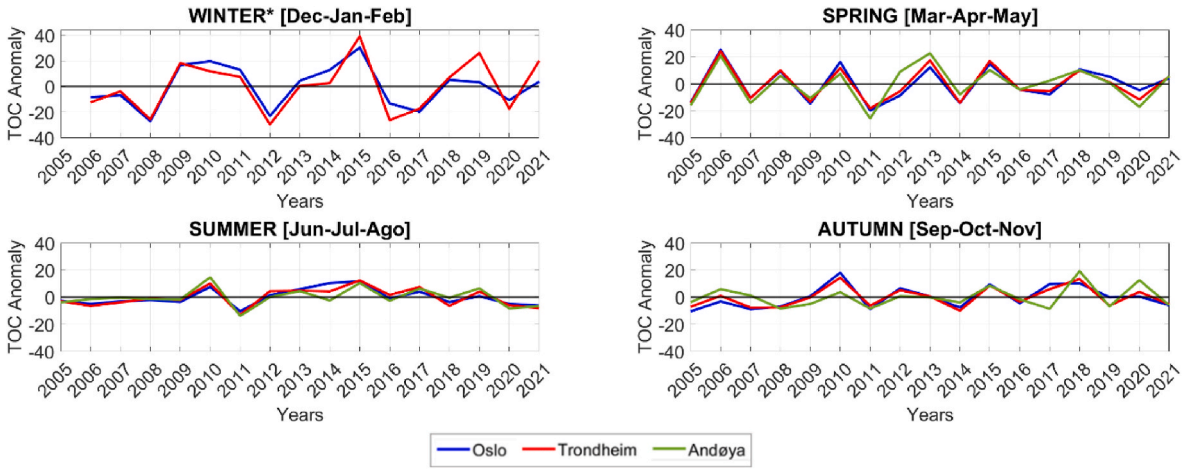

Fig. 2. Seasonal Total Ozone Column (TOC) anomalies trend for the three sites. *Several missing values in Andøya winter season did not allow to consider data in this evaluation. *This analysis was not performed for winter at Andøya due to the lack of data in this period.

(Manney and Lawrence, 2016; Johansson et al., 2019). The effect of the Arctic ozone depletion occurring in winter 2019/2020 (Manney et al., 2020) is also observed at the Norwegian sites here under study.

A clear greater variability of TOC amounts is visible in winter and spring, compared to summer and autumn as expected, primarily due to the short-term fluctuations (time scales of 1–3 days) on the TOC amounts associated with weather scale phenomena. To better investigated the role of the atmospheric circulation in the Norwegian region, the following analysis reported in this paper will be focused only on the months with larger TOC variability i.e., December–May period of each year.

3.2. Connection between GPH and TOC behaviour

Standardized seasonal TOC and GPH anomalies are shown in Fig. 3 for the winter and spring seasons. A significant anticorrelation among the two atmospheric parameters is observed during the spring season until 2016, the year after which it no longer occurs (pink solid line). In fact, from the year 2016, trends began to appear correlated, until the last observations of the year 2021. The reversal trend is especially visible during the spring months and considering this, the whole period has been divided into two-time intervals (i.e., from 2005 to 2016 and from 2016 to 2021) specifically looking at the winter and spring seasons over the whole period. The two time slots have been separately analysed by means of a correlation analysis reported in Fig. 3 thanks to which the temporal evolution of the statistic relationship among TOC and GPH parameters at the Norwegian sites has been investigated. In fact, a strong and statistically significant anticorrelation between total ozone and GPH was found for the interval 2005–2016 for Oslo and Trondheim stations (respectively −0.83 and −0.86) while a moderate anticorrelation (−0.52) was found in Andøya in the spring seasons (Table 2). In the interval 2016–2021 the Pearson (i.e., linear) correlation coefficients become positive among the two atmospheric parameters for all the Norwegian considered sites: high positive correlation for Andøya (0.67),

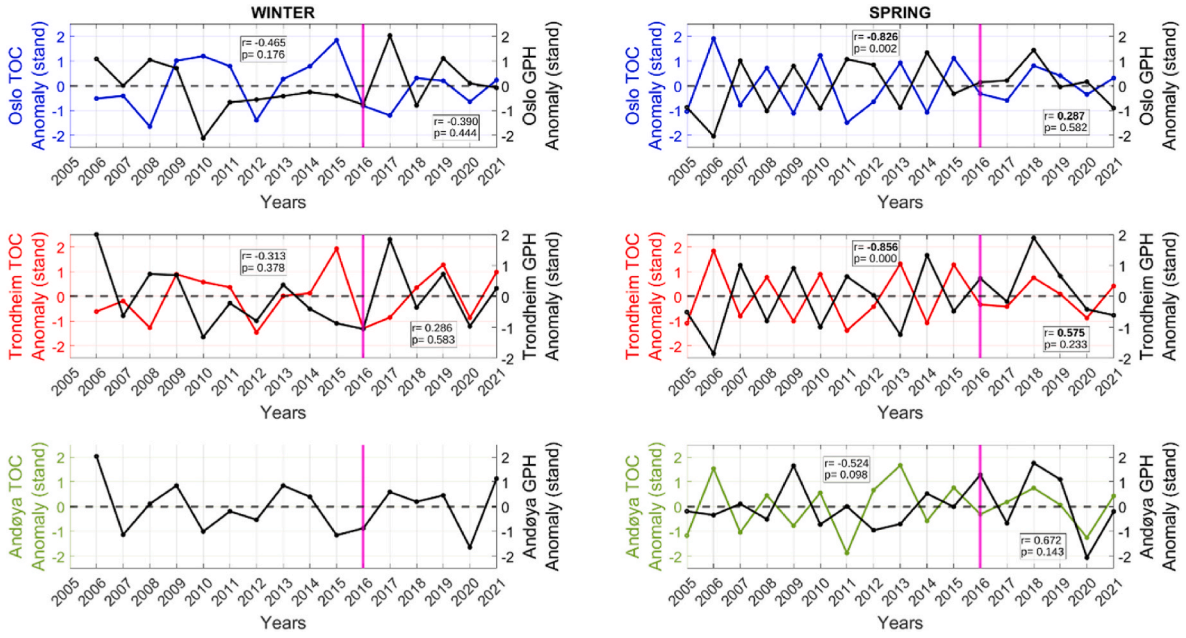

Fig. 3. Standardized seasonal TOC (coloured lines) and GPH (black lines) anomalies at Oslo (first row), Trondheim (second row) and Andøya (third row), in winter (first column) and spring (second column) seasons. Correlation coefficients (r) and related p-value (p) are reported both for the time interval before and after 2016 (pink solid line). The values are reported within boxes on the top and bottom areas of each plot, respectively. Correlations significant at the 0.05 level are reported in bold (p-value <0.05). *Several missing values in Andøya winter did not allow to consider data in this evaluation.

Table 2
Pearson correlation matrix: correlation coefficients between (**a**) the TOC and (**b**) the GPH monthly anomaly events for the pairs Oslo-Trondheim, Oslo-Andøya and Trondheim-Andøya over the period of interest. Correlation is always significant at the 0.05 level.

a) TOC anomaly	Oslo	Trondheim	Andøya	b) GPH anomaly	Oslo	Trondheim	Andøya[a]
Oslo	1	–	–	Oslo	1	–	–
Trondheim	.960	1	–	Trondheim	.921	1	–
Andøya	.732	.823	1	Andøya[a]	.662	.867	1

[a] No data available from 29 November to 13 January of each year for Andøya.

moderate correlation for Trondheim (0.57) and low but still positive correlation for the site of Oslo (0.29), even if in this case the p-values does not in any case reach the threshold of statistical significance (≤0.05) (Fig. 3). The anticorrelation between TOC and GPH parameters (so-well documented in literature) could have been attenuated from 2016 up to a reversal trend among the two parameters in the spring seasons. On the contrary, the reversal trend between TOC and GPH is weakly justified by the correlation analysis carried out on the winter months, since in this case the difference between the correlation coefficients before and after 2016 is not pronounced as in the case of the spring months. Moreover, the lack of data available for Andøya in the winter months hindered the possibility of comparison between the sites of interest. As a no significant change in volcanic activity around 2016 has been recorded, the physical process leading the weakening of the negative correlation between TOC and GPH remains uncertain.

In order to further understand the existing relationship between the occurrences of anomalies events in total ozone column and geopotential height values at 250 hPa in each different sites, and the existing association between them, we eventually used monthly anomalies instead of seasonal (as already described in Section 2.4). Table 2 shows the correlation analysis among the sites for the total ozone column monthly anomalies (a) and geopotential height monthly anomalies at 250 hPa (b) over the period December–May of the 17 considered years. The TOC and GPH at Oslo versus Trondheim show strong correlation coefficients equal to 0.960 for the total ozone column anomaly and 0.921 for geopotential height anomaly at 250 hPa suggesting that to a great extent the two sites are affected by the same synoptical systems. The corresponding correlations between the same variables at Andøya versus Trondheim are slightly weaker than previously (probably due to the larger distance, 676 km instead of 391.7 km) both for TOC anomaly (0.823) and for GPH anomaly (0.867). Finally, moderate statistically significant correlation was found between Andøya and Oslo for TOC (0.732) as well as for GPH (0.662), significant but still weaker than the other pairs as it was expected because of the largest distance between the two sites (1045.6 km).

With the aim of gaining more insights on the occurrences of significant TOC and GPH anomaly events at high-latitude we adopted the selection criterion ≥ +1σ or ≤ -1σ (of standardized TOC and GPH anomaly events). Standardized monthly anomalies determined in the period under study, which are above +1σ and below -1σ of TOC (green bins) and GPH (light blue bins) are shown in Fig. 4 (see Figure A1 in Appendix for more details). It is worth noting that the number of occurrences of significant TOC anomaly events increases with increasing latitude (more events in Andøya than in Trondheim and Oslo); while the number of occurrences of GPH anomaly events increases with decreasing latitude (more events in Oslo than in Trondheim and Andøya). In general, the higher number of TOC anomaly events compared to GPH, reflects the circumstances in which the ozone

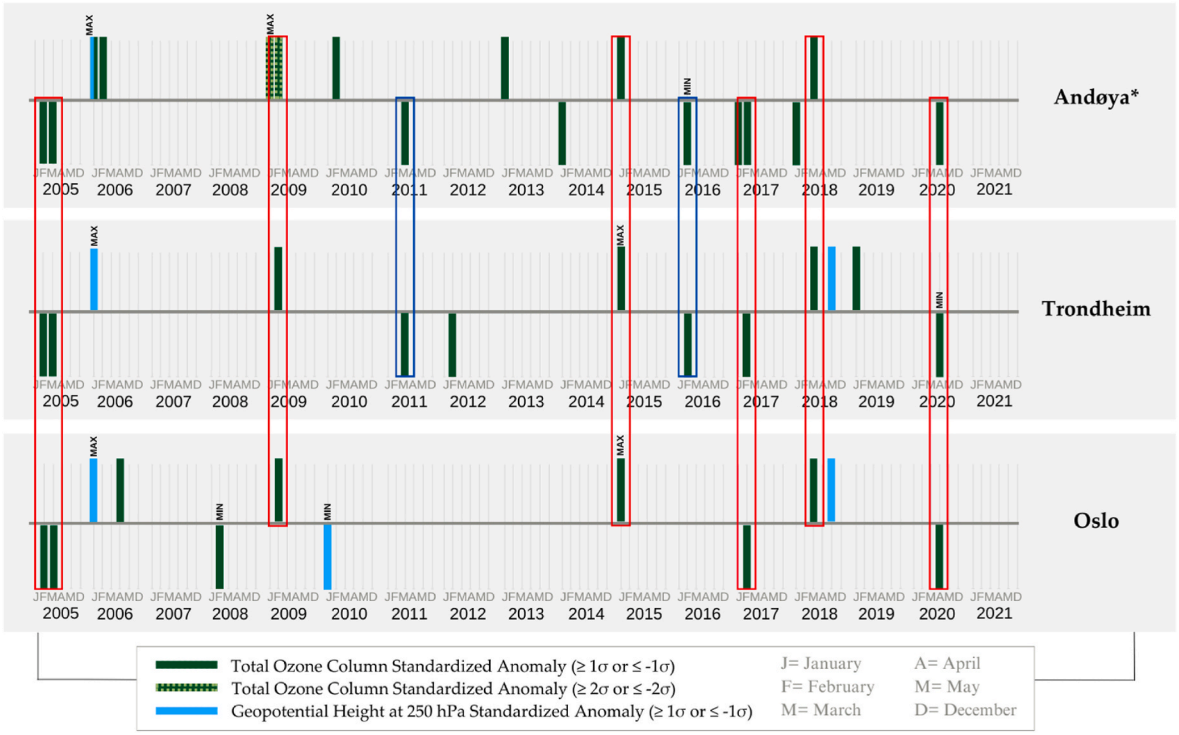

Fig. 4. Standardized monthly anomalies ≥ +1σ or ≤ -1σ and ≥ +2σ or ≤ -2σ of TOC (green bins) and GPH (light blue bins) over the period (January–December 2005/2021). Minimum and maximum occurrences for each variable are indicated with abbreviation "MIN" and "MAX". Red boxes highlight the cases in which TOC anomaly events in Andøya are concomitant to those at lower latitudes (Trondheim and Oslo). Blue boxes highlight other cases where TOC anomalies in Andøya occurred at the same time as in Trondheim, but not in Oslo. *No data available for Andøya in the time period from 29 November to 13 January of each year.

variability is more affected by other driving factors (i.e., ozone-poor air transport from polar zones), than by the geopotential height (Petkov et al., 2023). However, the number of events $\geq +1\sigma$ or $\leq$ -1σ is not relatively constant across the different Norwegian sites as it probably depends on the latitudinal distances between Oslo, Trondheim and Andøya. As already investigated by other authors (Fountoulakis et al., 2021; Friedel et al., 2022), the latitudinal gradient among different sites can result in substantial differences in the regional ozone trends. It is in fact known that ozone variability recorded for stations at higher latitudes (i.e., Andøya) are likely to be affected also by the polar ozone behaviour. Red boxes highlight the cases in which total ozone column anomaly events in Andøya occurred simultaneously to those happening at lower latitudes, in both Trondheim and Oslo (February 2005, March 2005, February 2017 and April 2020 for negative anomalies; February 2009, January 2015 and March 2018 for positive anomalies). Other cases where significant TOC anomaly appears over the same period only between Andøya and Trondheim (March 2011 and February 2016) are highlighted by means of blue boxes; this is likely due to the shorter latitudinal distance between Andøya and Trondheim, with respect to that between Andøya and Oslo. In one case (January 2006), the GPH anomaly events (at its maximum) are concomitant for all the considered sites also keeping the same sign. It can also be noted that extreme positive anomaly events ($\geq +2\sigma$) were only recorded in two cases (January–February 2009) during the entire period and only in the site of Andøya.

3.3. Association between TOC, teleconnection (TC) and solar activity

Three teleconnection indices (North Atlantic Oscillation, Arctic Oscillation and Scandinavia) have been examined in relation to geopotential height at 250 hPa and total ozone column at the Norwegian sites, Table 3 shows the Spearman correlation coefficients among the atmospheric parameters (TOC and GPH) and the teleconnection indices (NAO, AO and SCAND) referred to the monthly anomalies during the period of interest (December–May). The results shown in bold, highlight only for Oslo the statistical significance (p-value <0.05) between standardized TOC anomaly and NAO and AO Index. The correlations between standardized GPH anomaly and the examined teleconnection indices are also reported in the right side of Table 3. A clear predominant role of the SCAND Index is shown for the northern latitudes of Andøya and Trondheim, while other leading patterns (such as NAO and AO) are significant correlated (although the values are small) at Oslo. It is also important to take into account that NAO and AO patterns demonstrated (Ambaum et al., 2001) a high degree of temporal correlation, so this also affect the correlation with TOC and GPH. However, the visible difference among the northernmost latitudes and the Norwegian capital indicates that Andøya and Trondheim are influenced by a common circulation pattern, with respect from that of Oslo.

The occurrences of teleconnection indices and total ozone column anomaly events have been evaluated by adopting the same criterion as before ($\geq +1\sigma$ or $\leq$ -1σ and $\geq +2\sigma$ or $\leq$ -2σ). Fig. 5 reports standardized monthly TOC anomalies determined in the period under study for each of the different sites (rounded markers) and teleconnection indices (red and blue bins) and particularly displays only the occurrences of anomaly events which are above +1σ and below -1σ. The same figure also shows that the maximum solar activity represented by the yearly mean of solar radial flux (black solid line) happened in 2014. An increase in the NAO and AO positive phases (red bins), together with an increment of the SCAND negative phase (blue bins) are recorded starting from the significant sign change occurring at the beginning of the year 2015 (almost one year after the peak in solar activity - see Figure A2 in Appendix). Apart from this observation, nothing else remarkable can be deduced from the analysis of the annual trend of solar activity compared to the TC indices trends. This suggests the already investigated weak correlation between solar activity and teleconnection indices, as that inferred in Gray et al. (2013) where a lagged signal resembling a positive NAO response with respect to the solar maximum was found. While there is some evidence to suggest the occurrence of TC positive phases in delay with respect to maximum solar activity, the relationship is still not fully understood and requires further research. Regarding total ozone column, it is interesting to note that in cases where TOC anomalies occurred during the same period in all the sites considered (as it is shown in Fig. 4), there is a period of decreasing variation of solar activity. In fact, it can be observed that when solar activity tends to increase (from December 2009 to December 2013), there is a period during which there are far fewer occurrences of significant TOC anomalies and even a quiescence period for the lowest latitude considered (Oslo – blue markers in Fig. 5). The reversal trend since 2016 weakens the apparent good linear relationship found in the previous years, suggesting that other forcing factors (e.g., anthropogenic components) may be involved for better explaining the more complex relation between solar activity signature, climatic variables (e.g., TC indices) and total ozone (Scafetta and West, 2010).

Looking at the relationship among TC indices and TOC anomalies' trend over time it can be inferred that NAO index is in negative phase in the time period 2005–2011 when total ozone anomalies are mainly positive (this is especially true for Andøya, the site for which the greater number of significant anomaly events has been recorded). NAO index values together with TOC anomalies seem not to reach significance threshold of ±1σ in the period 2011–2014 except for few cases. After that, positive phase of NAO index begins to be observed in 2014 when TOC anomalies become mainly negative. Starting from spring 2020, NAO index again assumes negative values. The observations suggest that there exists a negative correlation among the two parameters, exceptions are: March 2005, January 2015 and April 2020. The same goes for the AO index, for which anomaly events more often reach higher (or lower) values (>2σ or <2σ) with respect to the NAO index. Again, AO index and TOC anomaly appear to be negatively correlated except for February–March 2005 and January 2015. The weak but negative correlation between TOC and NAO is already reported in literature by many authors who stated that pronounced and persistent positive phases of the NAO and AO indices are linked to total ozone depletion events in northern latitudes (Ossó et al., 2011; Appenzeller et al., 2000; Steinbrecht et al., 2011; Manney et al., 2011). Negative phases of SCAND

Table 3
Statistical parameters associated to the equations tested (among the atmospheric parameters and the teleconnection indices) for each of the three Norwegian sites during the period of interest (December–May). Spearman correlation coefficient (upper value) and probability value (lower value in brackets). Correlations significant at the 0.05 level are reported in bold (p-value <0.05).

Standardized monthly TOC anomaly	Oslo	Trondheim	Andøya[a]	Standardized monthly GPH anomaly	Oslo	Trondheim	Andøya
NAO	**−0.207** (0.037)	−0.183 (0.066)	−0.189 (0.088)	NAO	**0.211** (0.034)	0.056 (0.575)	0.128 (0.252)
AO	**−0.253** (0.010)	−0.176 (0.076)	−0.170 (0.126)	AO	**0.426** (0.000)	0.179 (0.072)	−0.005 (0.966)
SCAND	−0.102 (0.309)	−0.189 (0.057)	−0.132 (0.236)	SCAND	0.139 (0.163)	**0.348** (0.000)	**0.562** (0.000)

[a] No data available for Andøya in the time period from 29 November to 13 January of each year.

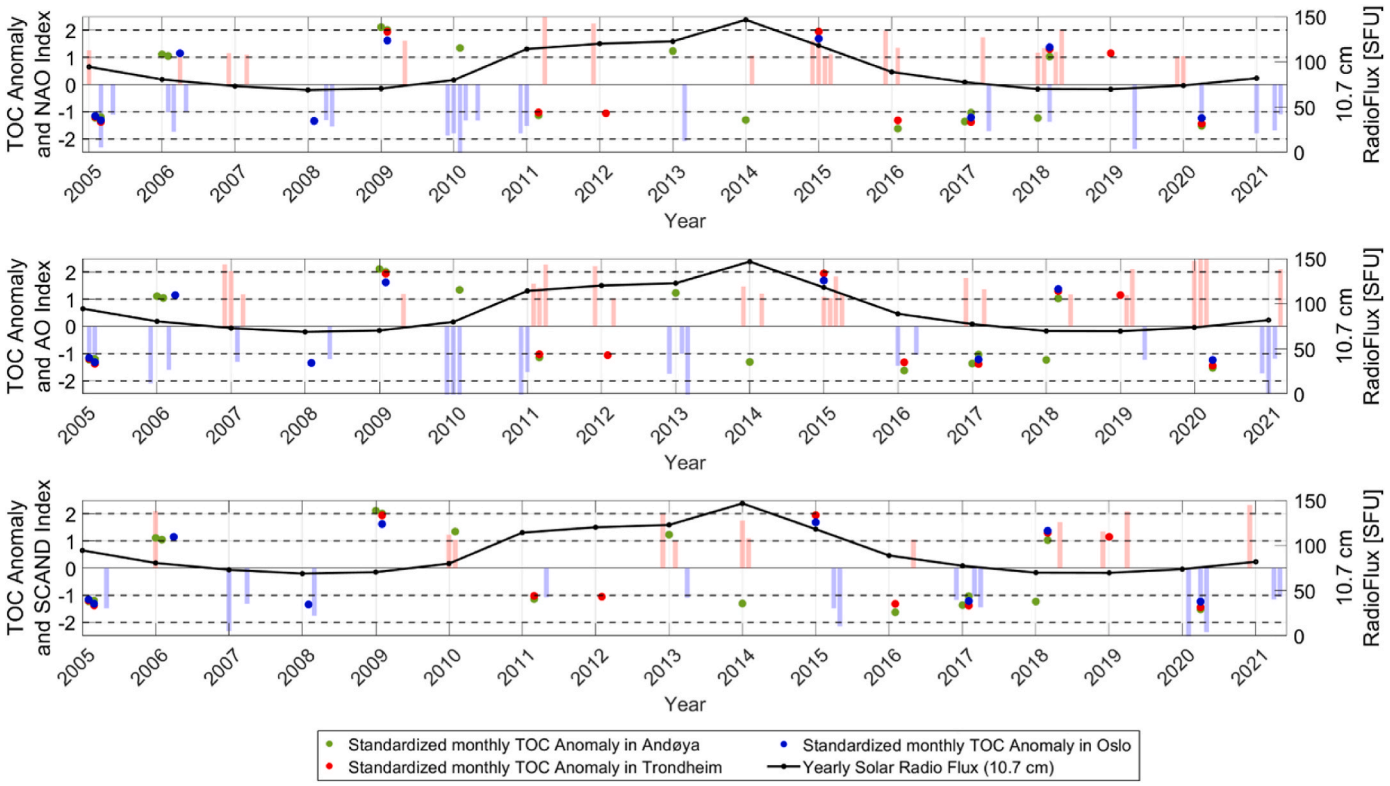

Fig. 5. Standardized monthly anomalies $\geq +1\sigma$ or $\leq$ -1σ of NAO (first row), AO (second row) and SCAND (third row) teleconnection indices (red and blue bins) and TOC (rounded markers) over the period (December–May 2005/2021) for the sites of Andøya (green); Trondheim (red) and Oslo (blue). Black solid line represents the yearly flux values from the Sun at a wavelenght of 10.7 cm.

index on the contrary coincide with negative anomalies of TOC. In addition, the SCAND index appears to show no significant changes ($>$ or $<$ than $\pm 1\sigma$) in conjunction with the minima in solar activity. Therefore, it can be inferred that where concurrent, TOC anomalies and significant changes in the SCAND index maintain the same sign, suggesting a quite different behavior than the other two indices described above.

4. Conclusion

In the present study, annual and multi-years total ozone column (TOC) variability at three different Norwegian sites was analysed considering its relationship with the geopotential height (GPH) at 250 hPa, the three Northern Hemisphere Teleconnection indices (NAO, AO and SCAND), and finally also with respect to the solar activity. Analyses were performed for Oslo, Trondheim and Andøya for which TOC measurements were retrieved from the polar satellite Aura. Severe ozone depletion events (i.e., 2011, 2016, 2020) recorded in the three sites was found to be in accordance with what already reported in literature.

The correlation between the GPH at the three sites, and between the TOC at the same three sites, showed that in both cases the strongest correlation existed for the combination Oslo-Trondheim (shorter latitudinal distance than all the other combinations). Weaker but still strong correlations were found between Trondheim and Andøya. Moderate but still significant correlations were found instead between Andøya and Oslo (larger latitudinal distance). In addition to the fact that there was a strong correlation between the monthly anomalies in GPH (and TOC) in Oslo, Trondheim and Andøya, the long-term trends in 2005–2021 at all three sites had the same sign (i.e., GPH and TOC were either increasing or decreasing at all sites) for most months of the year.

The results indicate that the temporal evolution of the statistical relationship among TOC and GPH parameters over the 17 years period, was characterized by a significant anticorrelation until 2016, the year after which a reversal trend was recorded leading to a positive linear correlation between the two atmospheric parameters. To further explore this behaviour, the occurrence of anomalies events in TOC and GPH data was evaluated thanks to the adoption of a filtering criterion. It was found that:

- TOC anomaly events increased with *increasing* latitude (more occurrences of $\geq +1\sigma$ and $\leq$-1σ standardized anomalies were recorded at Andøya than in the other two locations), while geopotential height at 250 hPa anomaly events increased with *decreasing* latitude (more occurrences of $\geq +1\sigma$ and $\leq$-1σ standardized anomalies were recorded at Oslo than in the other two locations).
- In most of the cases, TOC anomalies in Andøya occurred simultaneously to those at both the two lower latitudes, but other significant TOC anomaly events appear to be concomitant only between Andøya and Trondheim, suggesting a major connection between these two locations with respect to Oslo.
- When GPH anomalies ($\geq +1\sigma$ and $\leq$-1σ) are also recorded in Andøya and Trondheim (other than in Oslo), they appeared to be concomitant and also to keep the same sign than the lower latitude of Oslo.

Analysing the correlations among the atmospheric parameters (TOC and GPH) and the most prominent climatic modes of the Northern Hemisphere, it was found that the SCAND index has a prominent role in synchronizing TOC depletions when it is in its negative phase while at the opposite, TOC positive anomalies are more correlated with persistent positive phase of NAO index. SCAND index plays a clearly predominant role for the northern latitudes of Andøya and Trondheim while other leading patterns (such as NAO and AO) are significantly correlated (although the values are small) to the GPH recorded at Oslo. This difference among the northernmost latitudes and Oslo confirmed the previous insights on the major connection between Andøya and Trondheim, that are influenced by a common pattern, partially different from that of Oslo. Also, the analysis of solar activity suggested the existence of a

different behaviour in the Oslo anomalies events of TOC compared to those of Andøya and Trondheim: in fact, in the period of increasing variation of solar activity there were no significant TOC anomaly events recorded in Oslo (while on the contrary, they were recorded in Andøya and Trondheim).

Finally, this study explored the existing relationship among TC indices and total ozone column by investigating the occurrences of significant anomalies ($\geq+1\sigma$ or $\leq$-1σ) over the considered period of interest. The outcomes of the investigation confirmed the already stated weak but negative correlation among the North Atlantic Oscillation index and total ozone column anomalies, as well as among the Arctic Oscillation index and TOC anomalies for all the considered sites. On the other hand, the study highlighted that Scandinavia index has a quite different behaviour than the other two indices with respect to TOC anomaly trends; in fact, its positive significant changes coincide with positive TOC anomalies and vice versa.

CRediT authorship contribution statement

Giulia Boccacci: Methodology, Formal analysis, Data curation, Writing – original draft, preparation. **Chiara Bertolin:** Methodology, Writing – review & editing. **Stefano Cavazzani:** Methodology, data providing. **Anna Maria Siani:** Methodology, Writing – review & editing, All authors equally contributed to the conceptualisation of the manuscript, All authors have read and agreed to this version of the manuscript.

Declaration of competing interest

The authors declare that they have no known competing financial interests or personal relationships that could have appeared to influence the work reported in this paper.

Data availability

Data will be made available on request.

Acknowledgements

Part of the analyses used in this paper were produced with the Giovanni online data system, developed and maintained by the NASA GES DISC; the Ozone Processing Team of NASA is therefore acknowledged for the DOAS data. The authors are also grateful for the climate indices' data provided by the NOAA Climate Prediction Center. The authors thank the National Research Council of Canada for providing 10.7 cm solar radio flux data.

Appendix

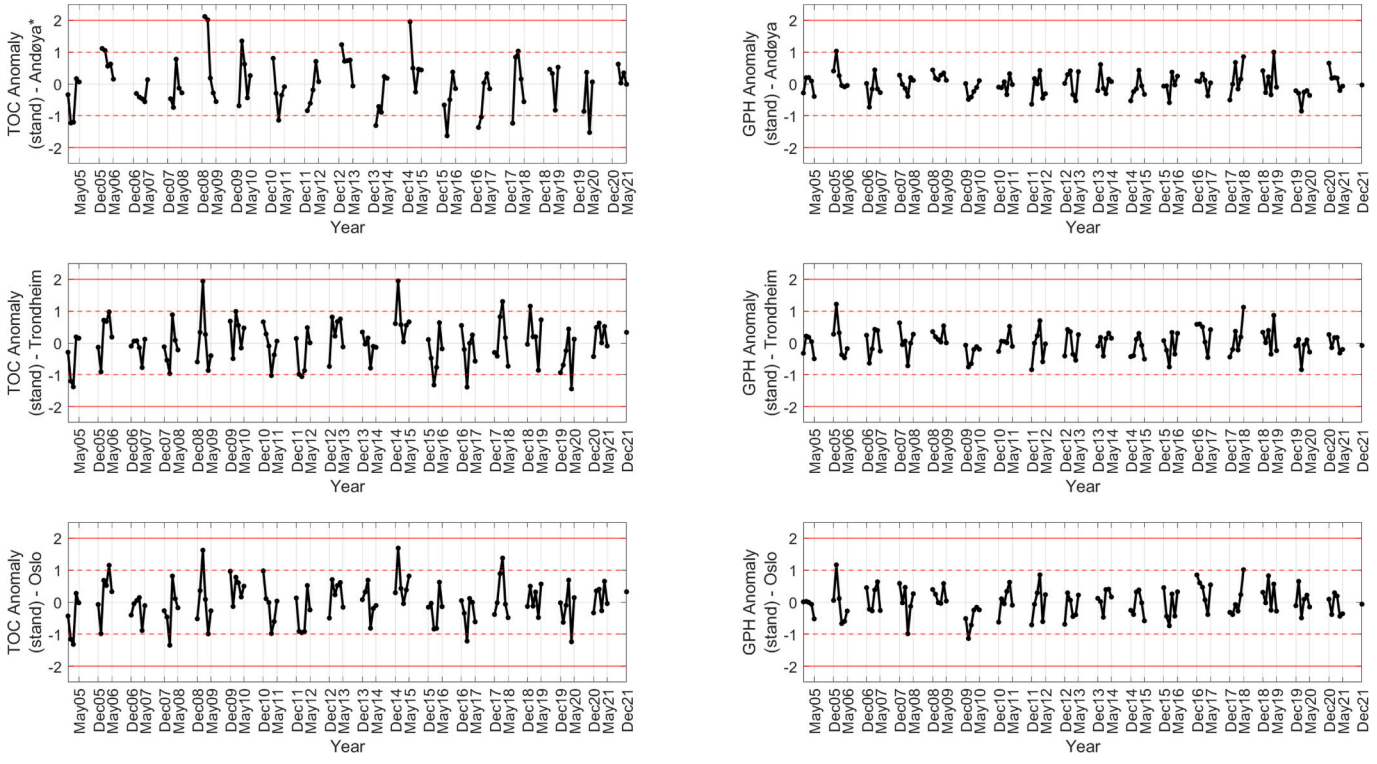

Fig. A1. Time plots of standardized TOC (first column) and GPH (second column) anomaly events over the period of interest (December–May 2005–2021), for the city of Andøya (first row), Trondheim (second row) and Oslo (third row). Thresholds at $\pm1\sigma$ (red dashed lines) and at $\pm2\sigma$ (red solid lines) indicate respectively significant and very high anomalous events. *No data available for Andøya in the time period from 29th November to 13th January of each year.

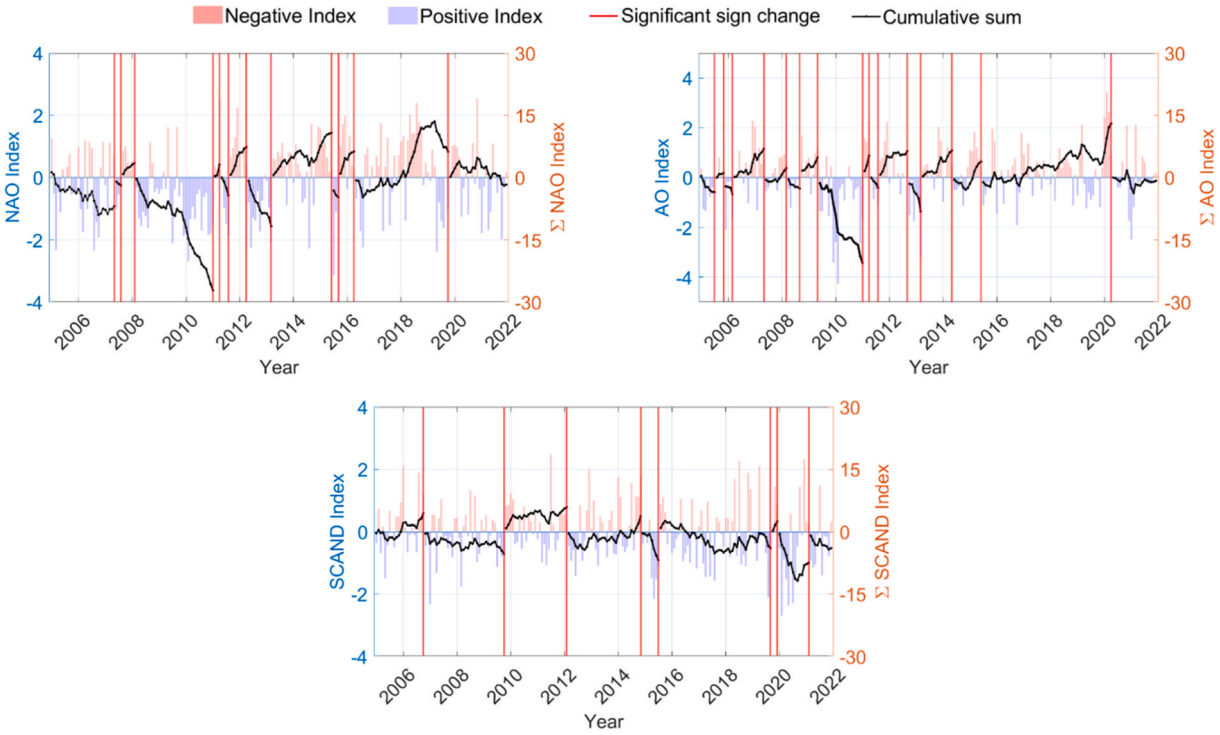

Fig. A2. (a) Time plots of NAO index, (b) AO index, and (c) SCAND index trends and corresponding cumulative curves (bold lines). The red solid lines highlight "significant" sign changes in the teleconnection indices trends. They are here defined as occurring when they are preceded and followed by the permanence of a positive or negative sign for at least 3 months (seasonal signal).

References

AIRS, 2019. Aqua/AIRS L3 Monthly Standard Physical Retrieval (AIRSonly) 1 Degree 1 Degree V7.0. Goddard Earth Sciences Data and Information Services Center, Greenbelt, MD, USA. https://doi.org/10.5067/UBENJB9D3T2H (GES DISC) [Data Set].

Ambaum, M.H.P., Hoskins, B.J., Stephenson, D.B., 2001. Arctic oscillation or North Atlantic oscillation? J. Clim. 14, 3495–3507.

Appenzeller, C., Weiss, A.K., Staehelin, J., 2000. North atlantic oscillation modulates total ozone winter trends. Geophys. Res. Lett. 27, 1131–1134. https://doi.org/10.1029/1999GL010854.

Baldwin, M.P., Dunkerton, T.J., 1979. Stratospheric harbingers of anomalous weather regimes. Science 294 (2001), 581–584.

Barnston, A.G.L.R.E., 1987. Classification, seasonality and persistence of low-frequency atmospheric circulation patterns. Mon. Weather Rev. 115, 1083–1126.

Bernet, L., Svendby, T., Hansen, G., Orsolini, Y., Dahlback, A., Goutail, F., Pazmiño, A., Petkov, B., 2023. Total Ozone Trends and Variability at Three Northern High-Latitude Stations. https://doi.org/10.5194/egusphere-egu22-3708.

Brönnimann, S., 2022. Century-long column ozone records show that chemical and dynamical influences counteract each other. Commun Earth Environ 3. https://doi.org/10.1038/s43247-022-00472-z.

Brönnimann, S., Schraner, M., Fischer, A., Brunner, D., Rozanov, E., Egorova, T., 2006. The 1986-1989 ENSO cycle in a chemical climate model. Atmos. Chem. Phys. 6, 4669–4685.

Climate Prediction Center. https://www.cpc.ncep.noaa.gov/data/teledoc/scand.shtml. (Accessed 31 March 2023).

Creilson, J.K., Fishman, J., Wozniak, A.E., 2005. Arctic oscillation-induced variability in satellite-derived tropospheric ozone. Geophys. Res. Lett. 32, 1–5. https://doi.org/10.1029/2005GL023016.

Dobson, G.M.B., Harrison, D.N., 1926. Measurements of the amount of ozone in the earth's atmosphere and its relation to other geophysical conditions. Proc. R. Soc. Lond. - Ser. A Contain. Pap. a Math. Phys. Character 110, 660–693.

Fountoulakis, I., Diémoz, H., Siani, A.M., Di Sarra, A., Meloni, D., Sferlazzo, D.M., 2021. Variability and trends in surface solar spectral ultraviolet irradiance in Italy: on the influence of geopotential height and lower-stratospheric ozone. Atmos. Chem. Phys. 21, 18689–18705. https://doi.org/10.5194/acp-21-18689-2021.

Frasca, F., Siani, A.M., Casale, G.R., Pedone, M., Bratasz, Strojecki, M., Mleczkowska, A., 2017. Assessment of indoor climate of mogiła abbey in kraków (Poland) and the application of the analogues method to predict microclimate indoor conditions. Environ. Sci. Pollut. Control Ser. 24, 13895–13907. https://doi.org/10.1007/s11356-016-6504-9.

Friedel, M., Chiodo, G., Stenke, A., Domeisen, D.I.V., Fueglistaler, S., Anet, J.G., Peter, T., 2022. Springtime arctic ozone depletion forces northern hemisphere climate anomalies. Nat. Geosci. 15, 541–547. https://doi.org/10.1038/s41561-022-00974-7.

GIOVANNI. The bridge between data and science v 4.38. Available online: https://giovanni.gsfc.nasa.gov/giovanni/. (Accessed 31 March 2023).

Gray, L.J., Scaife, A.A., Mitchell, D.M., Osprey, S., Ineson, S., Hardiman, S., Butchart, N., Knight, J., Sutton, R., Kodera, K., 2013. A lagged response to the 11 Year solar cycle in observed winter atlantic/European weather patterns. J. Geophys. Res. Atmos. 118 (13), 405–413. https://doi.org/10.1002/2013JD020062, 420.

Grooß, J.-U., Müller, R., 2022. Simulation of the record arctic stratospheric ozone depletion in 2020. Authorea Preprints. https://doi.org/10.1002/essoar.10503569.1.

Hansen, G., Svenøe, T., 2005. Multilinear regression analysis of the 65-year Tromsø total ozone series. J. Geophys. Res. Atmos. 110, 1–11. https://doi.org/10.1029/2004JD005387.

Hurrell, J.W., Kushnir, Y., Ottersen, G., Visbeck, M., 2003. An Overview of the North Atlantic Oscillation. In Geophysical Monograph Series, 134. Blackwell Publishing Ltd, pp. 1–35, 9781118669037.

Johansson, S., Santee, M.L., Grooß, J.U., Höpfner, M., Braun, M., Friedl-Vallon, F., Khosrawi, F., Kirner, O., Kretschmer, E., Oelhaf, H., et al., 2019. Unusual chlorine partitioning in the 2015/16 arctic winter lowermost stratosphere: observations and simulations. Atmos. Chem. Phys. 19, 8311–8338. https://doi.org/10.5194/acp-19-8311-2019.

Knibbe, J.S., Van Der A, R.J., De Laat, A.T.J., 2014. Spatial regression analysis on 32 Years of total column ozone data. Atmos. Chem. Phys. 14, 8461–8482. https://doi.org/10.5194/acp-14-8461-2014.

Koo, J.H., Wang, Y., Jiang, T., Deng, Y., Oltmans, S.J., Solberg, S., 2014. Influence of climate variability on near-surface ozone depletion events in the arctic spring. Geophys. Res. Lett. 41, 2582–2589. https://doi.org/10.1002/2014GL059275.

Lawrence, Z.D., Perlwitz, J., Butler, A.H., Manney, G.L., Newman, P.A., Lee, S.H., Nash, E.R., 2020. The remarkably strong arctic stratospheric polar vortex of winter 2020: links to record-breaking arctic oscillation and ozone loss. J. Geophys. Res. Atmos. 125 https://doi.org/10.1029/2020JD033271.

Liu, J., Rodriguez, J.M., Oman, L.D., Douglass, A.R., Olsen, M.A., Hu, L., 2020. Stratospheric impact on the northern hemisphere winter and spring ozone interannual variability in the troposphere. Atmos. Chem. Phys. 20, 6417–6433. https://doi.org/10.5194/acp-20-6417-2020.

Manney, G.L., Lawrence, Z.D., 2016. The major stratospheric final warming in 2016: dispersal of vortex air and termination of arctic chemical ozone loss. Atmos. Chem. Phys. Discuss. https://doi.org/10.5194/acp-2016-633.

Manney, G.L., Santee, M.L., Rex, M., Livesey, N.J., Pitts, M.C., Veefkind, P., Nash, E.R., Wohltmann, I., Lehmann, R., Froidevaux, L., et al., 2011. Unprecedented arctic ozone loss in 2011. Nature 478, 469–475. https://doi.org/10.1038/nature10556.

Manney, G.L., Livesey, N.J., Santee, M.L., Froidevaux, L., Lambert, A., Lawrence, Z.D., Millán, L.F., Neu, J.L., Read, W.G., Schwartz, M.J., et al., 2020. Record-low arctic stratospheric ozone in 2020: MLS observations of chemical processes and

comparisons with previous extreme winters. Geophys. Res. Lett. 47 https://doi.org/10.1029/2020GL089063.
Maria, A., Giuseppe, S., Casale, R., 2002. Investigation on a Low Ozone Episode at the End of November 2000 and its Effect on Ultraviolet Radiation.
Mateos, D., Antón, M., Sáenz, G., Bañón, M., Vilaplana, J.M., García, J.A., 2015. Dynamical and temporal characterization of the total ozone column over Spain. Clim. Dynam. 44, 1871–1880. https://doi.org/10.1007/s00382-014-2223-4.
Matthias, V., Dörnbrack, A., Stober, G., 2016. The extraordinarily strong and cold polar vortex in the early northern winter 2015/2016. Geophys. Res. Lett. 43 (12), 294. https://doi.org/10.1002/2016GL071676, 287-12.
Monge-Sanz, B.M., Casale, G.R., Palmieri, S., Siani, A.M., 2003. An investigation on total ozone over western mediterranean. Il Nuovo Cimento C 26, 53–60.
Okoro, E.C., Yan, Y. hua, Bisoi, S.K., Zhang, Y., 2021. Response and periodic variation of total atmospheric ozone to solar activity over mountain waliguan. Adv. Space Res. 68, 2257–2271. https://doi.org/10.1016/j.asr.2021.06.021.
Orsolini, Y.J., Doblas-Reyes, F.J., 2003. Ozone signatures of climate patterns over the euro-atlantic sector in the spring. Q. J. R. Meteorol. Soc. 129, 3251–3263. https://doi.org/10.1256/qj.02.165.
Ossó, A., Sola, Y., Bech, J., Lorente, J., 2011. Evidence for the influence of the North Atlantic oscillation on the total ozone column at northern low latitudes and midlatitudes during winter and summer seasons. J. Geophys. Res. Atmos. 116 https://doi.org/10.1029/2011JD016539.
Petkov, B.H., Vitale, V., Tomasi, C., Siani, A.M., Seckmeyer, G., Webb, A.R., Smedley, A. R.D., Casale, G.R., Werner, R., Lanconelli, C., et al., 2014. Response of the ozone column over Europe to the 2011 arctic ozone depletion event according to ground-based observations and assessment of the consequent variations in surface UV irradiance. Atmos. Environ. 85, 169–178. https://doi.org/10.1016/j.atmosenv.2013.12.005.
Petkov, B., Vitale, V., Di Carlo, P., Mazzola, M., Lupi, A., Diémoz, H., Fountoulakis, I., Drofa, O., Mastrangelo, D., Casale, G.R., et al., 2021. The 2020 arctic ozone depletion and signs of its effect on the ozone column at lower latitudes. Bulletin of Atmospheric Science and Technology 2. https://doi.org/10.1007/s42865-021-00040-x.
Petkov, B.H., Vitale, V., Di Carlo, P., Drofa, O., Mastrangelo, D., Smedley, A.R.D., Diémoz, H., Siani, A.M., Fountoulakis, I., Webb, A.R., et al., 2023. An unprecedented arctic ozone depletion event during spring 2020 and its impacts across Europe. J. Geophys. Res. Atmos. 128. https://doi.org/10.1029/2022JD037581.
Scafetta, N., West, B.J., 2010. Comment on "testing hypotheses about sun-climate complexity linking.". Phys. Rev. Lett. 105.
Schnadt, C., Dameris, M., 2003. Relationship between North Atlantic oscillation changes and stratospheric ozone recovery in the northern hemisphere in a chemistry-climate model. Geophys. Res. Lett. 30 https://doi.org/10.1029/2003GL017006.
Schwartz, M.J., Lambert, A., Manney, G.L., Read, W.G., Livesey, N.J., Froidevaux, L., Ao, C.O., Bernath, P.F., Boone, C.D., Cofield, R.E., et al., 2008. Validation of the Aura microwave limb sounder temperature and geopotential height measurements. J. Geophys. Res. 113 https://doi.org/10.1029/2007jd008783.
Solar radio flux - archive of measurements. Available online: https://www.spaceweather.gc.ca/forecast-prevision/solar-solaire/solarflux/sx-5-en.php. (Accessed 31 March 2023).
Solomon, S., 1999. Stratospheric ozone depletion: a review of concepts and history. Rev. Geophys. 37, 275–316.
Steinbrecht, W., Claude, H., Köhler, U., Hoinka, K.P., 1998. Correlations between tropopause height and total ozone: implications for long-term changes. J. Geophys. Res. Atmos. 103, 19183–19192. https://doi.org/10.1029/98JD01929.
Steinbrecht, W., Köhler, U., Claude, H., Weber, M., Burrows, J.P., Van Der A, R.J., 2011. Very high ozone columns at northern mid-latitudes in 2010. Geophys. Res. Lett. 38 https://doi.org/10.1029/2010GL046634.
Susskind, J., Barnet, C.D., Blaisdell, J.M., 2003. Retrieval of atmospheric and surface parameters from AIRS/AMSU/HSB data in the presence of clouds. IEEE Trans. Geosci. Rem. Sens. 41, 390–409. https://doi.org/10.1109/TGRS.2002.808236.
Svendby, T.M., 2004. Statistical analysis of total ozone measurements in Oslo, Norway, 1978–1998. J. Geophys. Res. 109. https://doi.org/10.1029/2004jd004679.
Svendby, T.M., Hansen, G.H., Bernet, L., Nilsen, A.-C., Schulze, D., Johnsen, B., 2021. Monitoring of the Atmospheric Ozone Layer and Natural Ultraviolet Radiation Annual Report.
Tapping, K.F., 2013. The 10.7 Cm solar radio flux (F10.7). Space Weather 11, 394–406. https://doi.org/10.1002/swe.20064.
Thompson, D.W.J., Wallace, J.M., 1998. The arctic oscillation signature in the wintertime geopotential height and temperature fields. Geophys. Res. Lett. 25, 1297–1300. https://doi.org/10.1029/98GL00950.
Tian, B., Manning, E., Roman, J., Thrastarson, H., Fetzer, E., Monarrez, R., 2020. AIRS V7 L3 Product User Guide AIRS Version 7 Level 3 Product User Guide AIRS V7 L3 Product User Guide.
Vaughan G, P.J.D., 1991. On the relation between total ozone and meteorology. Q. J. R. Meteorol. Soc. 117, 1281–1298.
Weather Spark Available online: https://it.weatherspark.com/y/148382/Condizioni-meteorologiche-medie-a-And%C3%B8ya-Andenes-Airport-Norvegia-tutto-l'anno (accessed on 31 March 2023).
Weber, M., Dikty, S., Burrows, J.P., Garny, H., Dameris, M., Kubin, A., Abalichin, J., Langematz, U., 2011. The brewer-dobson circulation and total ozone from seasonal to decadal time scales. Atmos. Chem. Phys. 11, 11221–11235. https://doi.org/10.5194/acp-11-11221-2011.
Weber, M., Coldewey-Egbers, M., Fioletov, V.E., Frith, S.M., Wild, J.D., Burrows, J.P., Long, C.S., Loyola, D., 2018. Total ozone trends from 1979 to 2016 derived from five merged observational datasets-the emergence into ozone recovery. Atmos. Chem. Phys. 18, 2097–2117.
Weber, M., Arosio, C., Coldewey-Egbers, M., Fioletov, V.E., Frith, S.M., Wild, J.D., Tourpali, K., Burrows, J.P., Loyola, D., 2022. Global total ozone recovery trends attributed to ozone-depleting substance (ODS) changes derived from five merged ozone datasets. Atmos. Chem. Phys. 22, 6843–6859. https://doi.org/10.5194/acp-22-6843-2022.
Wohltmann, I., von der Gathen, P., Lehmann, R., Maturilli, M., Deckelmann, H., Manney, G.L., Davies, J., Tarasick, D., Jepsen, N., Kivi, R., et al., 2020. Near-complete local reduction of arctic stratospheric ozone by severe chemical loss in spring 2020. Geophys. Res. Lett. 47. https://doi.org/10.1029/2020GL089547.
World Meteorological Organization, United States, 2018. National Oceanic and Atmospheric Administration; United States. National Aeronautics and Space Administration. United Nations Environment Programme; European Commission *Scientific Assessment of Ozone Depletion*, 9781732931718.
Zhang, J., Xie, F., Tian, W., Han, Y., Zhang, K., Qi, Y., Chipperfield, M., Feng, W., Huang, J., Shu, J., 2017. Influence of the arctic oscillation on the vertical distribution of wintertime ozone in the stratosphere and upper troposphere over the northern hemisphere. J. Clim. 30, 2905–2919. https://doi.org/10.1175/JCLI-D-16-0651.1.